Geochemistry of a Volcanic Hydrothermal System at Mount Spurr, Alaska

L. Garchar and R. Wendlandt

Colorado School of Mines, Golden CO
laura.garchar@gmail.com

Keywords
Exploration, geochemistry, Mt. Spurr, Alaska, stable isotopes

ABSTRACT

Mt. Spurr is an ice and snow-covered andesitic volcano located at the northern extent of the Aleutian arc in south central Alaska. Previous workers have identified a prospective geothermal system on the south side of the volcano. This research applies aqueous and mineralogical geochemical investigations at Mt. Spurr in order to characterize the hydothermal system, focusing on the possible extent, temperature, origin of fluids, and fluid pathways occurring in the system. Three spatially distinct endmember compositions have been identified: 1) moderate temperature (~50˚C), acidic, bicarbonate-poor, $d^{18}O$ and dD-enriched waters from Crater Lake, 2) low temperature (14-40˚C), neutral, bicarbonate and Mg-rich, slightly $d^{18}O$ and dD-enriched peripheral waters, and 3) cold (<9˚C), neutral, sulfate-rich, dilute/meteoric waters. Spring and seep waters sampled in this study represent shallowly circulating meteorically-derived waters that have variously interacted with rock, incorporated dissolved steam, possibly mixed with andesitic water, and been heavily diluted by cold meteoric water. Fluid pathways are likely controlled by local east-northeast and north-northeast and northwest trending faults that behave similarly to oblique-slip regional structures that bound the Cook Inlet. Permeability in andesitic flows that cover the field area is likely quite high, but clay minerals in weathered volcanic ash in between flows and in underlying Cook Inlet sediments likely act as barriers to deep circulation of meteoric water and upwelling of deeply sourced hydrothermal fluids. Precise mapping of fault structures that act as conduits to fluid flow and deeper drilling will enhance the understanding of the hydrothermal system at Mt. Spurr.

Introduction

Since at least the 1970's, it has been known that the state of Alaska has a number of proven or speculated geothermal resources (State Long Term Energy Plans 1980-1982, Turner and Wescott, 1986). However, due to the remote location of many potential geothermal fields and lack of energy transmission infrastructure, these resources have remained largely untapped.

Mt. Spurr is located about 100km west of Anchorage, in the Tordrillo Mountains on the northwest side of the Cook Inlet (Fig. 1). It is covered by about 67km^3 of perennial snow and ice, which is about 15 times more snow and ice than is present on Mount Rainier (Waythomas and Nye, 2002). Several valley glaciers dissect the volcano. Most of the area surrounding this volcano is uninhabited wilderness, and its remote location limits recreational use of the area (Waythomas and Nye, 2002).

Mt. Spurr's volcanic system has been widely studied by Alaska state agencies. Past and ongoing studies of gas emissions, ice melt, geologic history, seismic activity and geochemistry largely address the hazard of future eruptions. However, Mt. Spurr's recent volcanic activity and proximity to Anchorage also make it a prospective

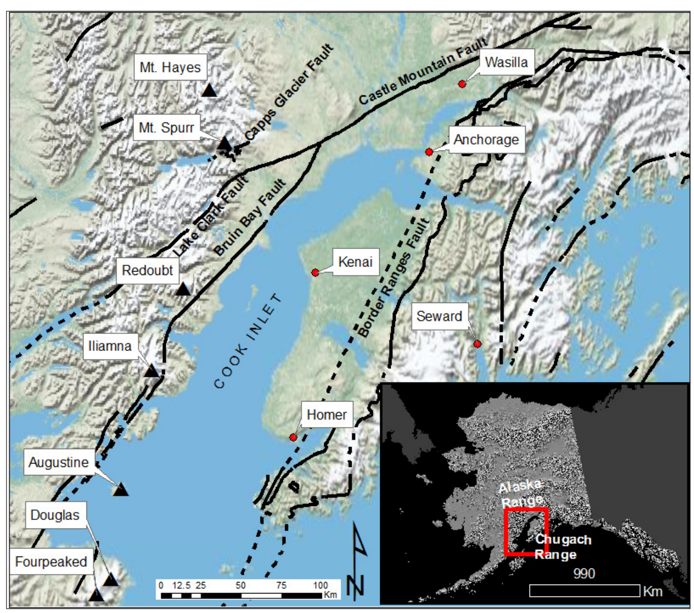

Figure 1. Mt. Spurr is in south-central Alaska on the eastern end of the Aleutian Arc. After Schaefer, 2006.

geothermal target. Turner and Wescott (1986) speculated that geothermal waters could be located south of Crater Peak at about 60m depth in porous tephra beds, and Martini et al.. (2011) have identified faults as well as magnetic, gravity and resistivity anomalies that could be related to the presence of a geothermal reservoir. This study examines the geochemistry of surface spring and seep waters collected over the summer of 2011, as well as published results.

Geologic Setting

The field area of this study is located on the south flank of Mt. Spurr, with the northern boundary at Crater Peak, the southern boundary at the Chakachatna River, the western boundary at Crater Glacier, and the eastern boundary just east of Chaka Ridge (Fig. 2).

Nye and Turner (1990) consider the andesitic lava flows that outcrop at Mt. Spurr, the Spurr volcanic complex (SVC), to be representative of eastern Aleutian volcanism. These authors also note that Mt. Spurr is the easternmost active volcano of the Aleutian arc, and it is located on the thickest crust of any Aleutian arc volcano. The SVC lies on top of continental crust formed by amalgamation of accretionary terranes including Silurian-early Jurassic limestone, basalt and clastic rocks, and Jurassic and/or Cretaceous flysch (Nye and Turner, 1990). All of these rocks have been intruded by the Alaska-Aleutian Range Batholith during Jurassic, early Tertiary, and mid-Teriary times (Reed and Lanphere, 1973). Immediately to the south of Mt. Spurr, the bedrock is granodiorite (62 and 69Ma), while to the north-northeast quartz monzonite intrudes Jurassic-Cretaceous flysch and is faulted against the West Foreland Formation (Nye and Turner, 1990). The West Foreland Formation is an Eocene tuffaceous sandstone and conglomerate unit that contains coal beds and underlies the oil and gas producing Kenai Group sediments in the Cook Inlet Basin (Montgomery and Barker, 2003).

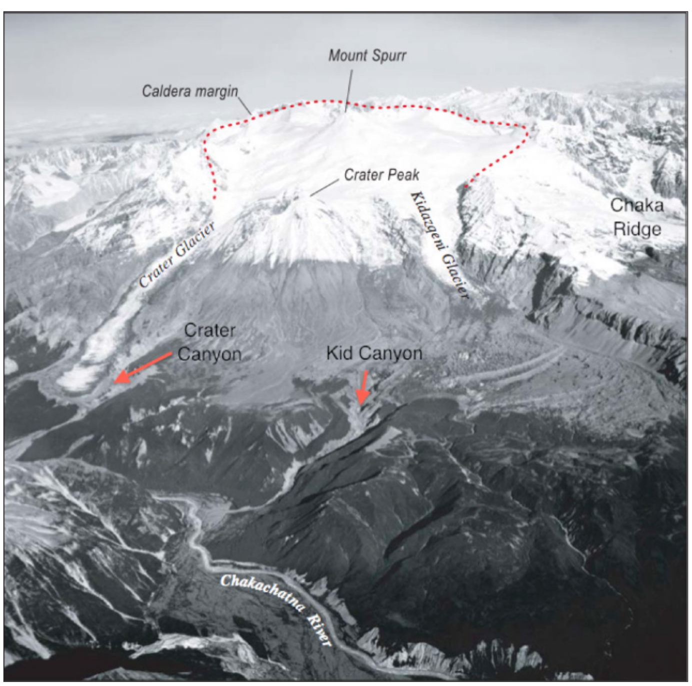

Figure 2. Air photo of Mt. Spurr, looking northwest, showing locations of Crater Peak, Crater Canyon, and Chaka Ridge. Core hole 26-11 is located just out of the field of view to the middle right. Modified from Waythomas and Nye, 2002.

Eruptive History

Tephra and lava flow deposits of the SVC show evidence of at least 35 eruptions in the last 6000 years (Riehle, 1985). The oldest lava flows and pyroclastic deposits at Mt. Spurr are around 255,000-18,000 years old. About 5800 years ago, the original edifice was destroyed in a Bezymianny-type eruption that produced a horseshoe-shaped caldera, a debris avalanche partially overlain by ash-flow tuff, and two new vents: the current Mt. Spurr, which grew out of the collapsed summit region, and Crater Peak, a breach on the south side of the edifice (Nye and Turner, 1990). Crater Peak erupted in 1953 and again in 1992. Both eruptions were Volcanian to sub-Plinian pyroclastic events that generated large volumes of volcanic ash (Waythomas and Nye, 2002).

Structures

Regional fault systems, including the reverse oblique-slip Castle Mountain, Lake Clark, and Bruin Bay faults (Fig. 1) have significant displacement (up to 1.2km reverse motion and 130km right lateral separation on the Castle Mountain Fault) and have been active in Eocene and more recent times (Finzel et al., 2009). However, the Castle Mountain fault is the only fault inferred to have Holocene motion (Finzel et al, 2009).

Just to the east of the study area, an exposure of the east-northeast trending, dextral-normal or transtensional Capps Glacier Fault (Figs. 1 and 3) juxtaposes Cenozoic granitic rocks to the northwest over gently deformed Cenozoic clastic rocks of the West Foreland Formation, to the southeast. The Capps Glacier Fault likely continues westward through the volcanic complex just to the south of Crater Peak (Wilson et al., 2009). Displacement could be tens to hundreds of meters (Finzel et al., 2009). Axes of folded Cenozoic basin deposits to the southeast of the Capps Glacier Fault are oriented 20-30˚ counterclockwise to the fault. Similar oblique

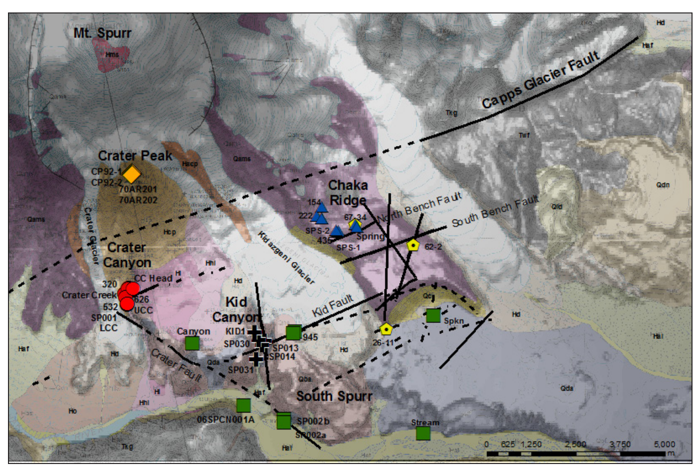

Figure 3. Sampling locations in the study area are shown over a geologic map from Nye and Waythomas, 2005. In this and subsequent figures, orange diamonds represent samples from Crater Peak (Crater Lake is located at Crater Peak), red circles are samples from Crater Canyon, blue triangles are samples from Chaka Ridge, black crosses are samples from Kid Canyon, green squares are samples from scattered locations to the south of Mt. Spurr, and yellow pentagons with black dots represent exploration core holes.

Table 1. Compiled water sampling at Mt. Spurr. Concentrations of cations, anions and major species are reported in mg/L, alkalinity in mg/L as $CaCO_3$, and conductivity in µmhos/cm. Isotopes are reported in units of per mil. Oxygen and hydrogen are relative to Vienna Standard Mean Ocean Water (VSMOW), sulfur relative to Vienna Canyon Diablo Troilite (VCDT), and carbon relative to Vienna Pee Dee Belemnite (VPDB). Samples with no reference were collected in this study.

	Date	T	pH	Alk	TDS	Cond	Na	Ca	K	Li	Mg	Cl	HCO3	SO4	B	F	Reference
Canyon	2011	3.8	6.43	54	300	520	200	32	5.3	<0.1	17	41	65	110	<0.1	0.23	
Canyon (replicate)	2011	3.8	6.44	54	310	520	25	33	5.2	<0.1	17	41	65	110	<0.1	0.24	
Stream	2011	9.1	6.79	11	140	200	5.6	20	1.4	<0.1	4.6	2.5	13	56	<0.1	<0.1	
945	2011	0	6.14	<1	10	6.6	<0.5	<0.5	<0.5	<0.1	<0.5	<0.1	<1	1.6	<0.1	<0.1	
945_10			8			1000						116	0	116			Ormat Nevada, 2012
Spurr Knob	2011		6.9				7.7	12	2.2		2.4	4.2	19	27		0.14	Ormat Nevada, 2012
SP002a	2010	18	4.9		38	47	3.2	6.4	1.5		2.8			7.2			Ormat Nevada, 2012
SP002b	2010	3	3.7		260	660	17	96	7.6		46	1.8		370		0.56	Ormat Nevada, 2012
CC Head	2011	6.9	5.72	<1	23	20	<0.5	1.9	<0.5	<0.1	<0.5	<0.1	<1	6.7	<0.1	<0.1	
626	2011	22.3	8.37	440	1200	1900	140	71	51	0.24	88	230	520	230	3.8	<0.1	
626 (replicate)	2011	22.3	8.33	440	1200	1800	150	76	52	0.25	89	210	530	220	4.1	0.46	
320	2011	12.2	5.89	1.4	74	120	3.3	11	1.1	<0.1	2.3	<0.1	1.8	43	<0.1	0.13	
Crater Creek	2011	14.5	7.88	340	830	1400	90	67	27	0.15	66	140	410	150	2.5	0.35	
SP001	2011	30.2	7.5	280	1400	2400	210	97	45	0.42	80	470	340	240	5.4	<0.1	
532	2011	22	7.52	350	1100	1800	140	82	37	0.27	75	260	430	180	3.8	0.44	
Crater Peak Hot Springs	1985	40.2	6.4		1708		266	95	75	0.42	99	254	622	477	7.7	1	Motyka & Nye, 1993
Upper Crater Creek	2005	23	7.63									320	238	150		0.56	Neal et al, 2008
Lower Crater Creek	2005	27.3	8.05									370	493	260		0.4	Neal et al, 2008
SP001	2010	41	7.04	310	1500	2100	210	100	45	0.4	79	470	320	240	5.7	0.61	Ormat Nevada, 2012
154	2011	0.2	6.24	2.2	20	34	1.1	2.5	0.66	<0.1	0.59	<0.1	2.6	9	<0.1	<0.1	
435	2011	3.3	6.24	1.5	27	32	0.89	2.8	<0.5	<0.1	<0.5	<0.1	1.8	9.7	<0.1	<0.1	
222	2011	0.8	6.51	2.9	27	41	1.4	3.8	0.54	<0.1	0.51	<0.1	3.5	12	<0.1	<0.1	
SPS-1	2011	0.1	6.47	3.2	11	37	1.4	3.4	0.67	<0.1	<0.5	<0.1	3.9	8.9	<0.1	<0.1	
SPS-2	2011	0.3	6.77	5.4	33	57	3.4	2.6	1.4	<0.1	1.6	<0.1	6.6	15	<0.1	<0.1	
Spring	2011	0.7	6.51	2.7	33	37	1.2	3.3	0.55	<0.1	<0.5	<0.1	3.3	10	<0.1	<0.1	
SPS-2_10	2010	1	6.92	4.8	42	57	3.5	2.7	1.7	<0.1	1.7	1	5.8	15	<0.1	<0.1	
SPS-1_10	2010	0	6.56	4.2	40	37	1.7	3.5	1	<0.1	0	1	5.1	9.7	<0.1	<0.1	
67-34	2010	30	8.44	80	600	150	34	29	12	<0.1	18	9.9	98	13	<0.1	0.42	
CP92-1	1992	49	2.48				56	184	3.51	0.034	40.5	53.2	0	1450	3.36	0.42	Keith et al, 1995
CP92-2	1992	49	2.49				55.1	187	3.69	0.035	41.3	54.5	0	1490	3.18	0.42	Keith et al, 1995
70AR-201	1970		2.17				75	192	7.5		71	1180	0	442	24		Keith et al, 1995
70AR-202	1970		2.3				75	182	7.3		70	1100	0	315	24		Keith et al, 1995
06SPCN001A	2006	12	8									116		122		0.54	Keith et al, 1995
KID1	2010	16	7.85	170	620	1000	89	55	12	0.16	35	140	200	130	0.2	0.52	Ormat Nevada, 2012
SP013	2010	1	7.54	30	200	230	36	80	5.2		9.8	25	36	40	0		Ormat Nevada, 2012
SP014	2010	11	7.94	97	440	670	75	87	10	0.13	35	83	120	89	0.13	0.31	Ormat Nevada, 2012
SP030	2010	16	6.92	200	540	900	72	51	7.2	0.18	52	92	250	110	0.22	0.35	Ormat Nevada, 2012
SP031	2010	17	6.84	180	540	810	60	47	6.5	0.16	46	82	210	110	0.16	0.46	Ormat Nevada, 2012

	Date	SiO2	Al	As	Ba	Fe	Mn	Sr	d18O	dD	d34S	d13C	Reference
Canyon	2011	50	<0.045	<0.005	<0.01	<0.01	<0.005	0.24	-18.5	-141.7	4.4	-10.5	
Canyon (replicate)	2011	48	<0.045	<0.005	<0.01	<0.01	<0.005	0.24	-18.6	-142.4	4.3		
Stream	2011	28	<0.045	<0.005	0.013	<0.01	<0.005	0.11	-16.5	-126.2	10.2	-9.3	
945	2011	0.63	<0.045	<0.005	<0.01	0.018	0.012	<0.1	-20.9	-157.9		-20.8	
945_10													Ormat Nevada, 2012
Spurr Knob	2011	36											Ormat Nevada, 2012
SP002a	2010	49	8.3		0.055	6.6	0.069						Ormat Nevada, 2012
SP002b	2010	75	130	0.011	0.55	130	2.8	0.78					Ormat Nevada, 2012
CC Head	2011	4.3	<0.045	<0.005	<0.01	<0.01	0.02	<0.1	-20.1	-153.8	0.5		
626	2011	92	<0.045	0.013	0.018	<0.01	0.057	0.57	-18.5	-148.1	8.4	-3.0	
626 (replicate)	2011	98	<0.045	0.013	0.02	<0.01	0.062		-18.5	-147.4	9.0		
320	2011	18	0.092	<0.005	0.011	0.021	0.016	<0.10	-19.6	-151.1	0.5		
Crater Creek	2011	78	<0.045	<0.005	0.022		0.016		-19.5	-152.3	8.1	-3.2	
SP001	2011	130	<0.045	0.022	0.044	0.032	0.34	0.92	-18.3	-147.3		-6.0	
532	2011	97	<0.045	<0.005	0.032	<0.01	<0.005	<0.1	-19.1	-151.2	8.7	-5.0	
Crater Peak Hot Springs	1985	125		0.021				0.68	-16.7	-138			Motyka & Nye, 1993
Upper Crater Creek	2005												Neal et al, 2008
Lower Crater Creek	2005												Neal et al, 2008
SP001	2010	130	0.12	0.03	0.051	0.46	0.62	0.91					Ormat Nevada, 2012
154	2011	7.9	<0.045	<0.005	<0.01	<0.01	<0.005	<0.1					
435	2011	9.3	<0.045	<0.005	<0.01	<0.01	<0.005	<0.1	-18.1	-137.2		-15.9	
222	2011	12	<0.045	<0.005	<0.01	<0.01	<0.005	<0.1	-18.6	-140	0.2	-6.5	
SPS-1	2011	11	<0.045	<0.005	<0.01	<0.01	0.022	<0.1	-18.1	-136.7	0.6	-6.7	
SPS-2	2011	16	<0.045	<0.005	<0.01	<0.01	<0.005	<0.1	-18.8	-141.6	2.2	-8.3	
Spring	2011	11	<0.045	<0.005	<0.01	<0.01	<0.005	<0.1	-18.0	-135.1	8.5	-9.2	
SPS-2_10	2010	17	<0.045	<0.005	<0.01	<0.01	<0.005	<0.1					
SPS-1_10	2010	12	<0.045	<0.005	<0.01	<0.01	<0.005	<0.1					
67-34	2010	100	46	<0.005	0.4	59	1.1	0.23					
CP92-1	1992	263	41.8	0.16		33.2	2.95		-116.0	-7.2			Keith et al, 1995
CP92-2	1992	312	50	0.26		31.6	2.94		-113.5	-7.2			Keith et al, 1995
70AR-201	1970												Keith et al, 1995
70AR-202	1970												Keith et al, 1995
06SPCN001A	2006												Keith et al, 1995
KID1	2010	97	18	0.0055	0.064	5.8	0.079	0.45					Ormat Nevada, 2012
SP013	2010	150	100		0.24	13	0.34	0.77					Ormat Nevada, 2012
SP014	2010	150	80		0.22	27	0.36	0.78					Ormat Nevada, 2012
SP030	2010	64	0.066		0.011			0.38					Ormat Nevada, 2012
SP031	2010	62						0.34					Ormat Nevada, 2012

orientations of cored anticlines in the Cook Inlet Basin could imply that the Bruin Bay, Castle Mountain, and Capps Glacier faults and associated folds evolved in similar regional stress conditions (Finzel et al., 2009). Surface elevation mapping, geophysical anomalies, and field studies suggest that several smaller E-NE and NW-trending faults that cross-cut the study area and likely influence fluid pathways (Martini et al., 2011).

Methods

Field Procedures

Water and core samples were collected at Chaka Ridge, South Spurr, and Crater Canyon areas during a field campaign 19 July-4 August 2011. Previous work including sampling from Martini et al. (2011) and helicopter-based field accessibility directed the selection of spring sampling locations. Sampling locations from this and previous work are shown in Fig. 3.

At each site, water was extracted by syringe and filtered through a 0.45μm membrane into a suite of bottles for laboratory geochemical analysis of anions, cations, major components, dissolved gas, and stable isotopes. The samples for cation analysis were acidified with 0.02N HNO_3. In addition, field H_2S, SiO_2, alkalinity, temperature, pH, and conductivity were measured. Approximate flow rate was estimated by visual observation.

Laboratory Procedures

Anions (Cl, B, F, HCO_3, SO_4), cations (Na, Ca, K, Li, Mg, Al, As, Ba, Fe, Mn, Sr), and major components (SiO_2, pH, Alk, TDS, Cond) were analyzed by the Western Environmental Testing Laboratory (WETLab) in Reno, NV. Stable oxygen, hydrogen, and sulfur (from sulfate) isotope analyses were conducted at the University of Nevada, Reno; and stable carbon isotope analyses were done at the University of Arizona.

Quality control procedures implemented by WETLab include running blanks, lab control samples, duplicates of client samples, and matrix spike samples. The results of these runs are within the acceptable parameters and have <5% relative difference. Charge balance calculations are <7% error with a few exceptions. "Canyon" has a 45% error, likely due to a concentration of Na that is an order-of-magnitude higher than the replicate. "945", "CC Head" and "435" also have high charge balance errors, likely because many of the constituents analyzed were below detection limit and therefore not included in the calculations. "Canyon," "945," "CC Head," and "435" are interpreted in light of these considerations.

Results

Water Chemistry

Analytical results from this research and published data are summarized in Table 1 and Figs 4-7. Most Mt. Spurr waters are neutral, bicarbonate or sulfate-rich, have high Mg relative to Na and K, are supersaturated with silica, and have an isotopic composition near meteoric water.

The $d^{13}C$ and $d^{34}S$ values of waters at Mt. Spurr range from -20.8‰ to -3‰ and 0.2‰ to 10.2‰, respectively. Samples from Crater Canyon cluster around $d^{13}C$ =-5‰, which suggests a contribution of carbon from a magmatic (as opposed to sedimentary or organic) source. Low Cl/SO_4 ratios in Spurr waters and a history of SO_4 scrubbing (Doukas and Gerlach, 1995) except during eruptions at Mt. Spurr suggest $d^{34}S$ fractionation due to oxidation of H_2S may be skewing $d^{34}S$ results, and that shallow equilibration is likely.

Water samples can be separated into three groups based on concentrations of chemical species: 1) moderate temperature (~50˚C), acidic, bicarbonate-poor, silica-rich, $d^{18}O$ and dD-enriched waters from Crater Lake, 2) low temperature (14-40˚C), neutral, bicarbonate, silica and Mg-rich, slightly $d^{18}O$ and dD-enriched peripheral waters, and 3) cold (<9˚C), neutral, sulfate-rich, dilute/meteoric waters. Peripheral waters include most samples from Crater Canyon and Kid Canyon; dilute/meteoric waters include most samples from Chaka Ridge. Samples from South Spurr lie somewhere between peripheral and dilute/meteoric compositions.

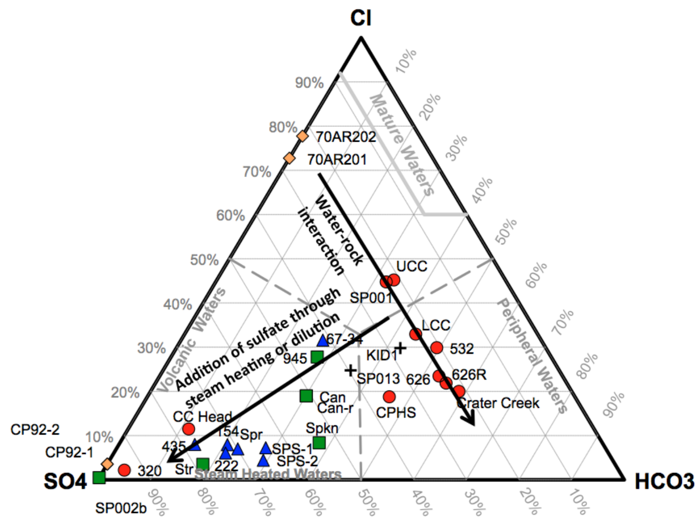

Figure 4. Anion ternary diagram showing most Spurr samples have high sulfate or bicarbonate content, indicating significant influence by shallow processes. Linear mixing trends between Crater Peak and Crater Canyon/Kid Canyon samples could represent water-rock interaction, and linear mixing trends between Crater Canyon and Chaka Ridge/South Spurr samples could indicate dilution/steam heating processes. Plot modified from spreadsheet by Powell, 2010.

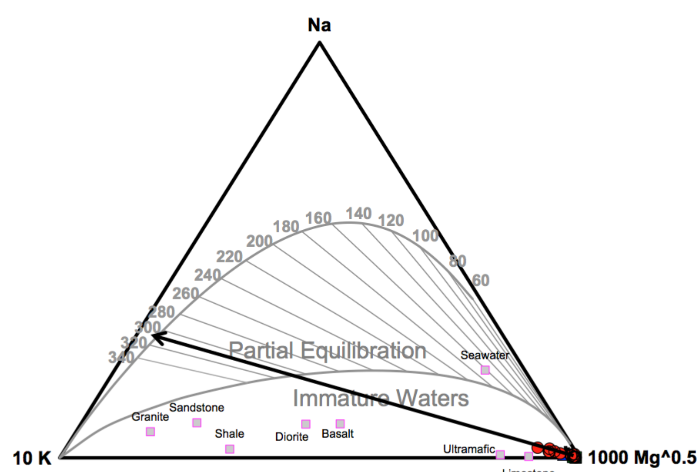

Figure 5. Cation ternary diagram showing Mg-rich composition of Spurr waters that are not in equilibrium with deep rock. A line drawn through samples extrapolates equilibrium temperature to ~310˚C. Plot modified from spreadsheet by Powell, 2010.

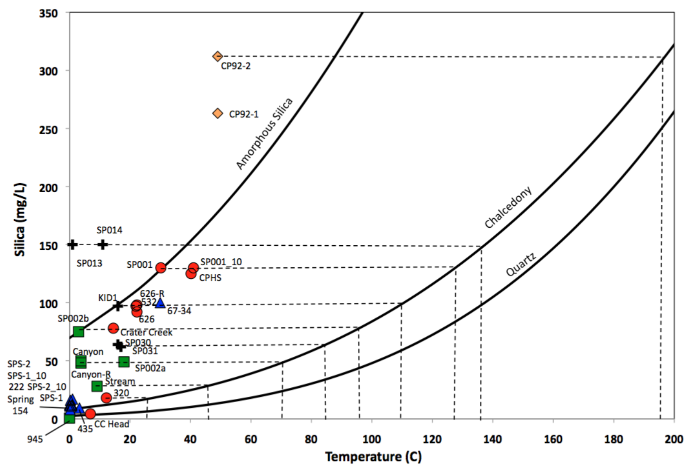

Figure 6. Sample temperature vs. silica content of Spurr waters. Low field temperatures of spring and seep waters indicate that chalcedony is probably the dominant silica phase. Most samples are supersaturated with respect to chalcedony, and extrapolating to the silica solubility curve yields original temperatures up to 155˚C for "SP001_10," and ~200˚C for "CP92-2."

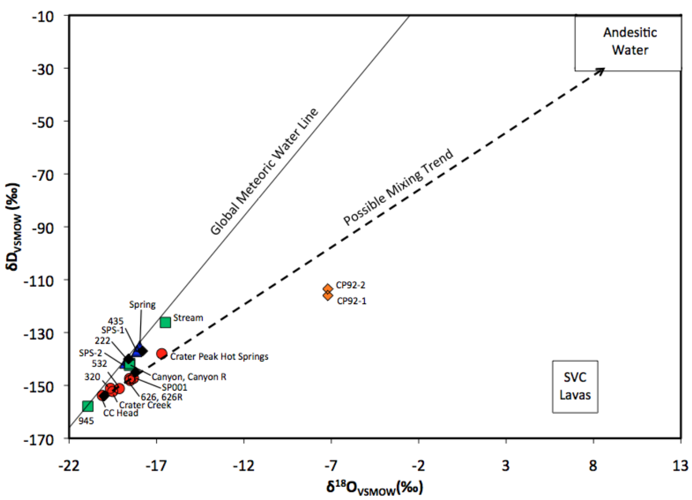

Figure 7. Stable oxygen and hydrogen isotopes of Spurr samples lie near the meteoric water line. Black diamonds represent cold stream or snow waters (Motyka and Nye, 1993). A shift in both $d^{18}O$ and dD cannot be accounted for by water-rock interaction alone. A positively sloping linear trend between Crater Canyon samples can be extrapolated to the composition of andesitic water ($d^{18}O$=10‰, dD=-20‰ from Giggenbach, 1992), suggesting a possible mixing trend between Crater Canyon samples and andesitic water. Crater Lake samples are likely enriched in $d^{18}O$ and dD due to evaporation. $d^{18}O$ of SVC lavas is from Nye and Turner, 1990, dD of SVC lavas is estimated.

Geothermometry

Solute geothermometer calculations (Fournier, 1979 and 1981; Truesdell, 1976; Giggenbach, 1988; Arnorsson, 1983; Tonani, 1980; Tonani, 1980; Nieva and Nieva, 1987; Fouillac and Michard, 1981; Kharaka et al., 1982; Kharaka and Mariner, 1989; Truesdess and Hulston, 1980) yield a wide range of deep (reservoir) temperature estimates, as shown in Fig. 8. Dilution likely causes the quartz estimate to be too low. Surface discharges at Mt. Spurr have lower Na but higher Ca and Mg than would be expected from a deep fluid. Na/K and Li/Mg geothermometers typically represent the highest temperature estimates, while K/Mg represents low estimates. Poor agreement between geothermometer calculations in addition to dilution, mixing, and shallow equilibration processes suggested by dissolved constituents in Spurr samples indicate the geothermometer temperature estimates do not reflect a deep reservoir temperature, but can give insight into shallow processes.

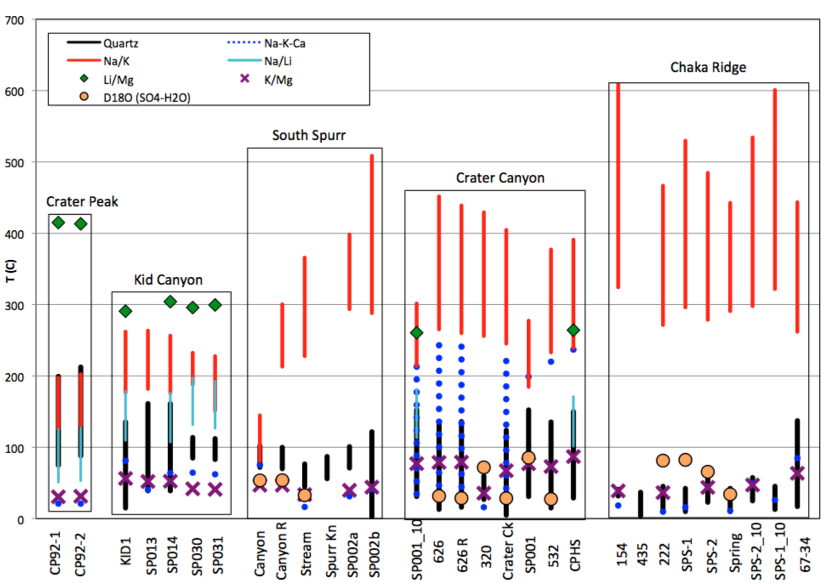

Figure 8. Solute geothermometer calculations for Spurr waters sometimes overlap but cover a wide range of estimates. Reasonable estimates of deep temperatures probably cannot be made from these surface discharges, but overlapping results indicate temperatures of last equilibration in the range of 100-200˚C at Crater Peak, 75-175˚C for sites south of Crater Peak, and 25-50˚C for Chaka Ridge

Discussion

Conceptual Model

Interpretations from this and previous research have been integrated into a conceptual model of the hydrothermal system at Mt. Spurr, as shown in Figures 8-9. In these figures, thicknesses of lithological units, placement of a magma body, and orientations of inferred structures are not well constrained. Arrows represent fluid pathways and a dot pattern represents boiling hydrtothermal fluids. The aforementioned water type classification scheme is spatially related to upflow and outflow of upwelling deep fluid and contributions of meteoric water from rain and snowmelt.

Mt. Spurr's position on an active convergent plate boundary provides a reliable heat source; active regional faults provide fractures and piles of porous volcanics provide permeability; abundant rain, snowmelt, and nearby seawater provide ample working fluid. Theoretically, a geothermal reservoir could be present in subsurface volcanic units capped by tephra, or in a presumed fractured granite basement that is capped by the West Foreland Formation. Geophysical anomalies confirmed by drilling in 2010-2011 (Martini et al., 2011) have shown secondary

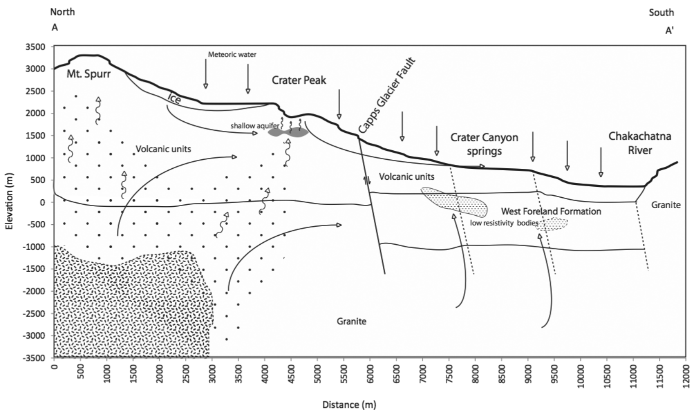

Figure 9. Conceptual N-S cross-section of field area from Mt. Spurr summit to the Chakachatna River. The pattern in the bottom left corner represents a magma body, dot pattern represents boiling fluid, and arrows indicate direction of fluid flow. Seeps in Crater Canyon are fault-controlled and represent shallowly circulating meteoric water that seems to be mixing with Crater Lake or andesitic water.

argillic to advanced argillic alteration and slickenlines on faults at Chaka Ridge and clay altered fault zones and clay intervals to the south of Chaka Ridge, which indicates fluid flow has occurred at shallow depths in the past. Yet exploration drilling in this area has not encountered temperatures above 57˚C at 1km depth (Ormat Nevada, 2012).

The West Foreland Formation encountered in two exploration core holes contains beds of montmorillonite and has extensive calcite replacement of sandstone and conglomerate matrix as well as calcite veining that cross-cuts clasts. Detrital grains are deformed by compaction and there is very little porosity. It is possible that this unit acts as a seal that prevents water percolating down from overlying volcanics from circulating deep enough to be influenced by magmatic processes, and also prevents deep hydrothermal fluid from upwelling to the surface, except along faults. The entire thickness of the West Foreland Formation in the study area is unknown and has not been penetrated by drilling. Future studies of the hydrothermal system at Mt. Spurr would benefit from a more complete understanding of the stratigraphy of the study area, especially of what lies beneath the West Foreland Formation. This would allow the hypothesis that there is a geothermal reservoir capped by the West Foreland Formation to be tested.

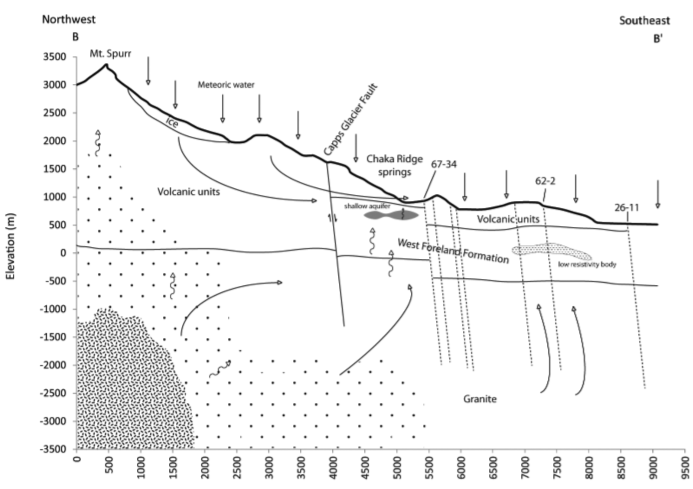

Figure 10. Conceptual NW-SE cross-section of field area from Mt. Spurr summit through Chaka Ridge. Patterns are the same as Fig. 9. Seeps on Chaka Ridge are topographically controlled and represent shallow circulation of meteoric water through porous volcanics and minor incorporation of steam.

Summary

The concentrations of dissolved constituents and isotopic composition of surface discharges at Mt. Spurr indicate that these waters do not directly represent potential geothermal reservoir fluid. Some evidence of deep circulation or upwelling hydrothermal fluid can be found in peripheral and Crater Lake waters, but these have been heavily diluted with meteoric and shallow groundwater. The hydrologic framework and extent of a possible geothermal reservoir are influenced by subsurface lithology, which is only known to 1km depth in the study area. It appears that deep hydrothermal fluid does not reach the surface, except along faults, and this may be due to a cap of clay-mineral rich West Foreland Formation sediments that lie below porous volcanics and basement. Precise mapping of fault structures that act as conduits to fluid flow and deeper drilling will enhance the understanding of the hydrothermal system at Mt. Spurr.

Acknowledgements

Ormat and the State of Alaska for providing funding and field access. Allison Payne, Matt Uddenberg, Robert Stephan, Brad Peters, and Manuel Barros for field assistance.

References

Arnorsson, S. (1983). Chemical equilibria in Icelandic geothermal systems. Implications for chemical geothermometry investigations. *Geothermics* 12 119-128.

Doukas, M. P. and Gerlach, T. M. (1995). Sulfur dioxide scrubbing during the 1992 eruptions of Crater Peak, Mount Spurr volcano, Alaska. *USGS Bulletin* 2139.

Finzel, E. S., Gillis, R. J., Ridgway, K. A., and LePain, D. L. (2009). Preliminary evaluation of basin margin exhumation and provenance of Cenozoic strata, Chuitna and Beluga rivers area, Cook Inlet forearc basin, Alaska. Alaska Division of Geological and Geophysical Surveys Preliminary Interpretive Report 2009-4.

Fouillac, C. and Michard, G. (1981). Sodium/lithium ratio in water applied to geothermometry of geothermal reservoirs. *Geothermics* 5 41-50.

Fournier, R. O. (1981). "Application of water geochemistry to geothermal exploration and reservoir engineering" in *Geothermal Systems: Principles and Case Histories.* New York, NY: Wiley.

Fournier, R. O. (1979). Geochemical and hydrological considerations and the use of enthalpy-chloride diagrams in the prediction of underground condiditons in hot spring systems. *Journal of Volcanology and Geothermal Research* **5** 1-16.

Giggenbach, W. F. (1992). Isotopic shifts in waters from geothermal and volcanic systems along convergent plate boundaries and their origin. *Earth and Planetary Science Letters* **113** 495-510.

Giggenbach, W. F. (1988). Geothermal solute equilibria. Derivation of Na-K-Mg-Ca geoindicators. *Geochimica et Cosmochimica Acta* **52** 2749-2765.

Keith, T. E. C., Thompson, M. T. and McGimsey, R. G. (1995). Chemistry of Crater Lake waters prior to the 1992 eruptions of Crater Peak, Mount Spurr volcano, Alaska. *USGS Bulletin 2139.*

Kharaka, Y. K., Lico, M. S., and Law, L. M. (1982). Chemical geothermometers applied to formation waters, Gulf of Mexico and California basins. *AAPG Bulletin* 66 588.

Kharaka, Y. K. and Mariner, R. H. (1989). "Chemical geothermometers and their application to formation waters from sedimentary basins" in *Thermal History of Sedimentary Basins: Methods and Case Histories.* New York, NY: Springer-Verlag.

Martini, B.A., Lide, C., Owens, L., Walsh, P., Delwiche, B., Payne, A. (2011) Geothermal Resource Definition at Mt. Spurr, Alaska. *Geothermal Resources Council Transactions* 35.

Montgomery, S. L., and Barker, C. E. (2003). Coalbed methane, Cook Inlet, south-central Alaska: A potential giant gas resource. AAPG Bulletin, v. 87, 1, 1-13.

Motyka, R.J. and Nye, C.J. (1993) Fumarolic gas chemistry (1982) and thermal spring water chemistry, crater peak (1985), Mount Spurr, Alaska. *Short Notes on Alaskan Geology.* Alaska Department of Geological and Geophysical Survey Professional Report 113.

Neal, C. A., McGimsey, R. G., Dixon, J. P., Manevich, A., and Rybin, A. (2008). 2006 Volcanic activity in Alaska, Kamchatka, and the Kurile Islands: summary of events and response of the Alaska Volcano Observatory. *USGS Scientific Investigations Report 5214.*

Nieva, D. and Nieva, R. (1987). Developments in geothermal energy in Mexico, part 12-A cationic composition geothermometer for prospection of geothermal resources. *Heat recovery systems and CHP* 7 243-258.

Nye, C.J., and Turner, D.L. (1990). "Petrology, geochemistry and age of the Spurr Volcanic Complex, eastern Aleutian arc," *Bulletin of Volcanology*, **5**2, 205–226.

Ormat Nevada, Inc., 2012; Drill records, logs, reports from Mt. Spurr Geothermal Exploration; Wells 26-11, 62-2, 67-34; Tyonek Quadrangle, Alaska: Alaska Division of Geological & Geophysical Surveys Geologic Materials Center Data Report (pending).

Powell, T., Cumming, W. (2010). Spreadsheets for geothermal water and gas geochemistry. *Proceedings, Thirty-Fifth Workshop on Geothermal Reservoir Engineering, Stanford University* SGP-TR-188.

Reed, B. L. and Lanphere, M. A. 1973. Alaska-Aleutian Range Batholith: geochronology, chemistry and relation to circum-pacific plutonism. *GSA Bulletin* 84 2583-2610.

Riehle, J. R. (1985). A reconnaissance of the major Holocene tephra deposits in the Upper Cook Inlet region, Alaska. *Journal of Volcanology and Geothermal Research* 37 74.

Tonani, F. (1980). Some remarks on the application of geochemical techniques in geothermal exploration. *Proc. Adv. Eur. Geoth. Res. Second Symposium, Strasbourg,* 428-443.

Truesdell, A. H. (1976). Summary of Section III. Geochemical techniques in exploration. *Proceedings 2nd UN Symposium on the development and use of geothermal resources, San Francisco, 1975* 1 liii-lxxix.

Truesdell, A. H. and Hulston, J. R. (1980). "Isotopic evidence on environments of geothermal systems" in *Handbook of Environmental Isotope Geochemistry*: Elsevier.

Turner, D.L., and Wescott E.M. (1986). "Geothermal energy resource investigations at Mt. Spurr, Alaska," Geophysical Institute of the University of Alaska UAG R-308.

Waythomas, C.F., and Nye, C.J. (2002). "Preliminary volcano-hazard assessment for Mount Spurr volcano, Alaska," USGS OFR 01-482.

Wilson, F. H., Hults, C. P., Schmoll, H. R., Haeussler, P. J., Schmidt, J. M., Yehle, L. A., and Labay, K. A. (2009). Preliminary geologic map of the Cook Inlet region, Alaska. *USGS OFR 2009-1108.*